RI 9260

REPORT OF INVESTIGATIONS/1989

Effect of Energy and Impact Direction on Coal Fragmentation

By Jon I. Voltz

BUREAU OF MINES

UNITED STATES DEPARTMENT OF THE INTERIOR

Mission: As the Nation's principal conservation agency, the Department of the Interior has responsibility for most of our nationally-owned public lands and natural and cultural resources. This includes fostering wise use of our land and water resources, protecting our fish and wildlife, preserving the environmental and cultural values of our national parks and historical places, and providing for the enjoyment of life through outdoor recreation. The Department assesses our energy and mineral resources and works to assure that their development is in the best interests of all our people. The Department also promotes the goals of the Take Pride in America campaign by encouraging stewardship and citizen responsibility for the public lands and promoting citizen participation in their care. The Department also has a major responsibility for American Indian reservation communities and for people who live in Island Territories under U.S. Administration.

Report of Investigations 9260

Effect of Energy and Impact Direction on Coal Fragmentation

By Jon I. Voltz

UNITED STATES DEPARTMENT OF THE INTERIOR
Manuel Lujan, Jr., Secretary

BUREAU OF MINES
T S Ary, Director

Library of Congress Cataloging in Publication Data:

Voltz, Jon I.
Effects of energy and impact direction on coal fragmentation.

(Report of investigations; 9260)

Supt. of Docs. no.: I 28.23:9260.

1. Blasting. 2. Impact. 3. Blast effect. I. Title. II. Series: Report of investigations (United States. Bureau of Mines) ; 9260.

TN23.U43 [TN279] 622 s [622'.334] 88-607919

CONTENTS

	Page
Abstract	1
Introduction	2
Experimental design	2
Experimental equipment	3
Discussion of results	4
Summary	7
Appendix A.–Energy distribution for parallel and perpendicular impacts	8
Appendix B.–Particle size distribution for parallel and perpendicular impacts	10
Appendix C.–ANOVA summary for dependent variables	11
Appendix D.–ANOVA program	12
Appendix E.–Input energy determination for pendulum impactor	13
Appendix F.–Student's t-values of paired data	14
Appendix G.–Summary of student's t-numbers and confidence levels for 3/8-in and 150-mesh screens	15
Appendix H.–Summary of airborne respirable dust generated on impact	16

ILLUSTRATIONS

1. Sample enclosure method for particulates and dust retrieval	3
2. Impact test pendulum machine	3
3. Screening results for all input energies parallel and perpendicular to bedding plane	5
4. Relationship between fragmentation-input energy ratio and nominal input energy	6

TABLES

1. Average particle size distribution for parallel and perpendicular impacts	4
2. Generation of minus 150-mesh dust and ARD by parallel and perpendicular impacts	4
3. Average energy distribution for parallel and perpendicular impacts	4
4. Parallel and perpendicular impact particles passing 3/8-in mesh	6

UNIT OF MEASURE ABBREVIATIONS USED IN THIS REPORT

deg	degree	lb	pound
°F	degree Fahrenheit	μm	micrometer
ft	foot	mg/m^3	milligram per cubic meter
ft•lbf	foot pound (force)	min	minute
ft/s^2	foot per square second	pct	percent
h	hour	scfh	standard cubic foot per hour
in	inch	wt pct	weight percent

EFFECT OF ENERGY AND IMPACT DIRECTION ON COAL FRAGMENTATION

By Jon I. Voltz[1]

ABSTRACT

The U.S. Bureau of Mines has conducted fundamental coal fragmentation studies to evaluate the effects of impact energy and direction of bedding planes on dust generation, size distribution, and impact-output energy relationships. Product size distributions were obtained for the fragmented samples by screening to minus 150 mesh. The minus 150-mesh fines were analyzed with a light scattering photometer with a measurement range of 176 to 1.9 μm. Increased input energy produced a significant increase in the weight of plus 3/8-in material for impact perpendicular to the bedding planes. No significant trend was observed for parallel impact. Impact direction had little influence on dust size distribution, and input versus output energy relationships. As expected, total airborne dust measured at time of impact and percent particulates below 11 μm in size generally increased with increased input energy for both directions of impact. Energy used for sample fragmentation increased with increased energy input.

[1]General engineer, Twin Cities Research Center, U.S. Bureau of Mines, Minneapolis, MN.

INTRODUCTION

The objective of this work was to establish the relationship of impact energy applied parallel and perpendicular to the bedding planes to fragment size distribution, airborne dust generation, and energy absorbed by fragmentation. To be able to design mechanized mining techniques to recover coal with minimum fine particle and airborne dust generation, the design engineer must first understand the fragmentation process of the material being mined.

In 1975, Kurth, Sundae, and Shultz published a report[2] on coal size distributions as a result of fragmentation by drop, impact, compression, and shear tests. They used six energy levels and measured coarse fragments, nonairborne and airborne fines, and respirable airborne fractions. The impact tests were done using a pendulum mass system with input energies of 95, 164, 223, 293, 365, and 455 ft•lbf. The impact fragmentation results nominally showed an equal distribution percentage across the size ranges, but the total particle count for fines and dust increased with increased impact energy. However, a comparison of experimental forces applied with actual cutting forces suggested that the impact energies used were far too high for coal. Additionally, the 2- by 2- by 4-in samples used in the previous work were all prepared with bedding planes perpendicular to the direction of impact along the 4-in axis.

A new pendulum impact tester was designed and built with the impact point at the center of percussion instead of the center of gravity as done in the previous experiment. The center of percussion impact point does not lose energy to the pendulum frame as a center of gravity impact does. Additionally, the new device was fully instrumented for on-line data analysis by computer to minimize operator error.

The new system required approximately one-third the input energy of the old system to produce the same fragment size distribution.

This difference was attributed to sample impact location and pivot center friction. The new pendulum machine reduced pivot friction to 1 ± 0.2 pct of input force with a ball-bearing mount. The current test series used center of percussion instead of center of gravity for impact center point.

EXPERIMENTAL DESIGN

A 2 by 5 test matrix was used for the experiment, with eight replications for each test. The independent variables in the tests were impact energy and impact orientation. Five energy levels were used, 10, 25, 40, 55, and 70 ft•lbf, with two directions of impact, perpendicular and parallel to the bedding plane of the test samples. The samples used were 2-in cubes of Illinois No. 6 coal. Static compressive tests were not run.

After the samples were cut to the size desired for testing, they were placed in plastic boxes containing some water and sealed. The samples were then stored in a refrigerator at a temperature of $33° \pm 1°F$ until needed for testing. This storage technique was intended to minimize both oxidation and moisture loss from the samples.

The sample was removed from storage and taken out of the box approximately 2 h prior to the test, allowing ample time for it to dry and reach room temperature. For the test, the sample was resealed in a dry plastic bag, to contain all dust and particles generated by impacting, and placed between the platens of the test system (fig. 1).

The dependent energy variables measured for each test were (1) energy retained in the striking bob, (2) energy lost through the test sample to the backing bob, (3) energy lost to friction, and, (4) sample fragmentation energy. The ratio of the energy absorbed in fracturing the sample to the input energy, the fragmenting-input energy ratio, measures the efficiency of fracture for a given sample orientation. Other dependent variables were total airborne dust produced on impact, size distribution of the fragment products from 1/2-in to 150 mesh (106 μm), and percent fines from the minus 150-mesh screening bottoms cumulative to 11 μm, expressed as a fraction of the original sample weight. Friction in the pendulum system of 1 ± 0.2 pct of input force was so low it was ignored in the analysis.

The Tyler screens used were 1/2 and 3/8 in, 3, 5, 9, 20, 35, 60, 100, and 150 mesh. The coal fragments were hand sifted through 8-in-diameter screens of 1/2-in, 3/8-in, and 3-mesh openings. The particles passing 3 mesh were sifted through a stack of 3-in-diameter screens of 5-, 9-, 20-, 35-, 60-, 100-, and 150-mesh openings. An air vibrator agitated the stack without passing air through the screens. The screen agitator was run for 1 min for each run using ≈100 scfh air feed.

[2]Kurth, D. I., L. S. Sundae, and C. W. Schultz. Dust Generation and Comminution of Coal. BuMines RI 8068, 1975, 28 pp.

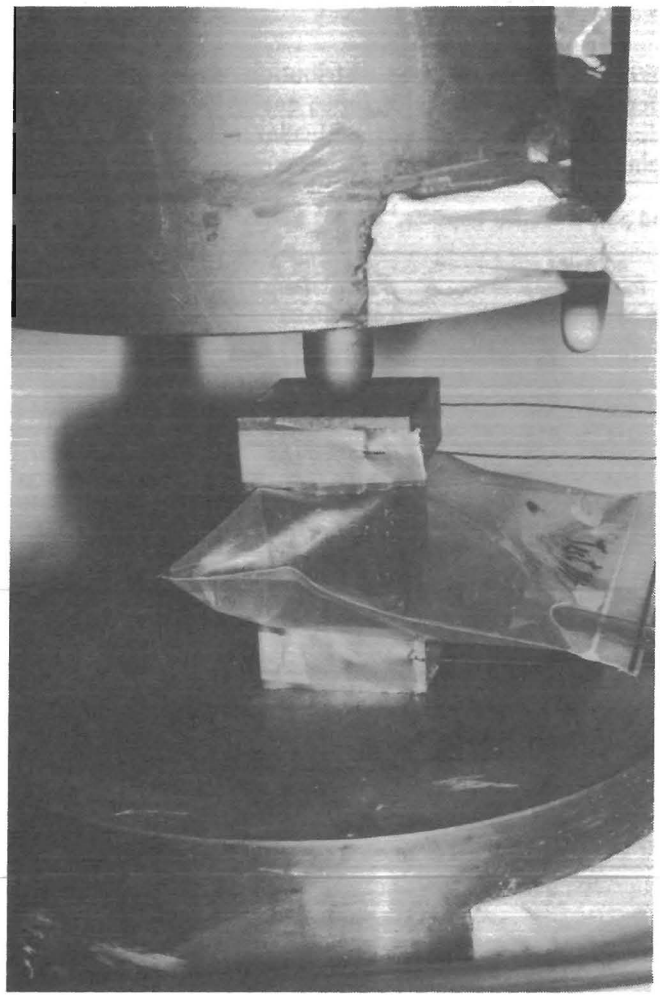

Figure 1.–Sample enclosure method for particulates and dust retrieval.

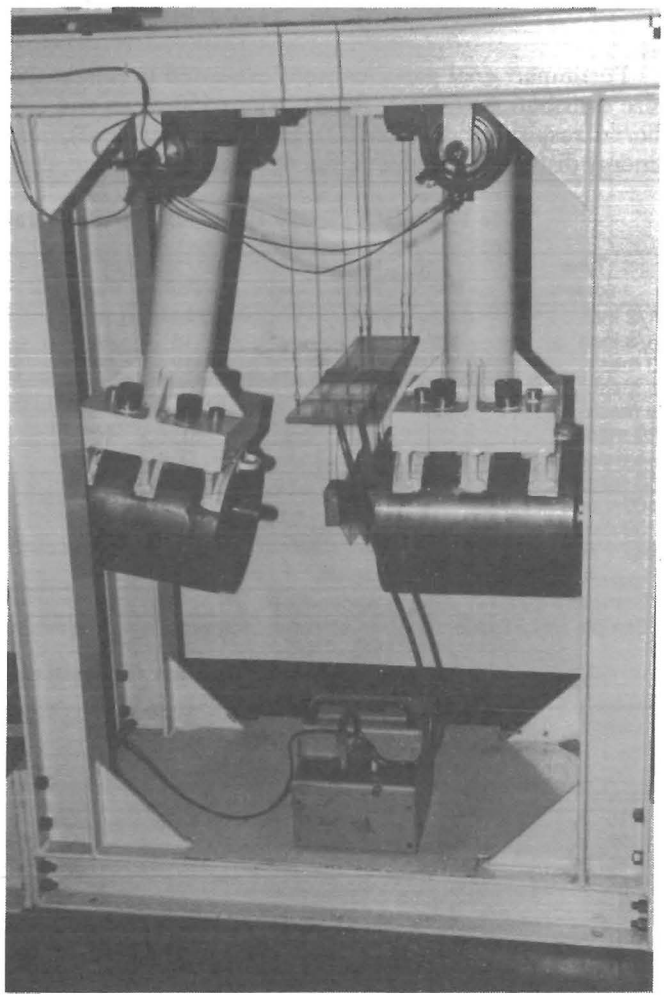

Figure 2.–Impact test pendulum machine.

EXPERIMENTAL EQUIPMENT

The impact test equipment was designed with a pair of free swinging adjacent pendulums mounted on bearings held in a support frame. Design and operating data for the pendulum impactor are contained in appendix E. A hemispherical impactor was affixed to the center of percussion[3] of the striking pendulum on the bob face. A space was allowed between the two adjacent cylinder bob faces to accommodate the impactor and the suspended, bagged 2-in-coal cube, which was mounted between a pair of suspended, hardened plates (fig. 2). The hardened plates were used to distribute the impact energy uniformly through the sample instead of as a point load.

The suspended assembly of bagged sample and plates was secured to the receiving pendulum with elastic bands. The plastic bag holding the sample was connected to an exhaust tube leading to a GCA[4] model RAM-l real-time aerosol monitor (RAM) that was used to measure the airborne respirable dust (ARD) generated by the impact. The monitor sample transport system passes aerosol 9 μm and smaller.

A series of 10 Tyler screens from 1/2 in to 150 mesh were used to analyze the large postimpact particles. A commercially available laser beam, light scattering, particle sizing system was used for size analysis of postimpact minus 150-mesh fines.

[3]The center of percussion is the distance from the pivot center that can be struck without adding a force vector to the pivot center. This distance is the product of the natural period (t^2) and the gravitational constant (32.167 ft/s^2) divided by $4\pi^2$.

[4]Reference to specific equipment does not imply endorsement by the U.S. Bureau of Mines.

DISCUSSION OF RESULTS

Postimpact coal particles were evaluated to obtain the size distribution (table 1, fig. 3), minus 150-mesh and airborne respirable dust (ARD) generation (table 2), and energy distribution (table 3, fig. 4). Size distribution, dust generation, and energy distribution were compared to determine the effects of input energy levels and impact direction–parallel and perpendicular to the sample bedding plane.

Table 1.–Average particle size distribution for parallel and perpendicular impacts,[1] weight fraction passing[2]

Tyler screen	10 ft•lbf		25 ft•lbf		40 ft•lbf		55 ft•lbf		70 ft•lbf	
	Par	Perp	Par	Perp	Par	Perp	Par	Perp	Par	Perp
1/2 inch	0.07	0.03	0.28	0.19	0.35	0.31	0.45	0.33	0.33	0.42
3/8 inch	.05	.018	.18	.13	.26	.22	.31	.24	.21	.31
3 mesh	.03	.014	.12	.096	.17	.16	.21	.17	.14	.22
5 mesh	.02	.032	.05	.046	.05	.067	.08	.08	.07	.09
9 mesh	.009	.004	.028	.025	.029	.037	.039	.035	.028	.034
20 mesh	.003	.0016	.011	.009	.011	.014	.015	.013	.011	.012
35 mesh	.002	.0008	.006	.005	.007	.008	.009	.007	.006	.007
60 mesh	.001	.0004	.0033	.0026	.004	.0042	.0047	.0037	.0035	.0033
100 mesh	.0005	.0002	.0016	.0013	.0017	.0022	.0022	.0017	.0017	.0016
150 mesh	.0003	.0001	.0008	.0007	.001	.0012	.0014	.0011	.0010	.0009

Par Parallel.
Perp Perpendicular.
[1]Complete data set given in appendix B.
[2]Sample weight entering given screen minus sample weight retained by that screen divided by starting sample weight (sum of fractions).

Table 2.–Generation of minus 150-mesh dust and ARD by parallel and perpendicular impacts

Direction and impact energy, ft•lbf	Minus 150-mesh, 10^{-3} wt pct[1]		ARD, mg/m^3	
	Average	SD	Average	SD
Parallel:				
10	4.5	NA	2.3	1.9
25	6.4	0.8	9.2	5.8
40	7.9	3.6	8.6	7.7
55	9.2	2.5	14	10
70	5.8	2.3	21	11
Perpendicular:				
10	2.7	NA	1.9	2.8
25	6.6	2.2	6.2	3.4
40	9.3	1.9	15	10
55	9.1	3.1	17	12
70	4.7	2.0	32	12

ARD Airborne respirable dust.
NA Not available.
SD Standard deviation.
[1]Cumulative 1.9- to 11-μm particulates.

Table 3.–Average energy [1] distribution for parallel and perpendicular impacts[2]

Impact, ft•lbf, and direction	Energy, ft•lbf			Ratio[3]	Absorbed energy, ft•lbf
	Input	Retained	Fragmenting		
10:					
Parallel	10.09	0.72	5.3	0.52	4.1
Perpendicular	10.07	.07	4.3	.42	5.8
25:					
Parallel	25.01	3.6	15.9	.64	5.5
Perpendicular	25.02	2.4	15.6	.63	7.0
40:					
Parallel	40.16	7.1	24.7	.61	8.4
Perpendicular	40.00	5.7	24.3	.61	10.0
55:					
Parallel	55.00	10.3	36.0	.65	8.8
Perpendicular	54.95	9.8	29.6	.56	14.3
70:					
Parallel	69.98	14.1	39.6	.57	16.5
Perpendicular	69.87	14.9	40.0	.57	15.0

[1]Complete data set given in appendix A.
[2]Fragmenting energy–energy used in sample breakage; absorbed energy–backup bob response; retained energy–energy not spent in sample breakage or in backup bob response.
[3]Fragmenting energy to input energy.

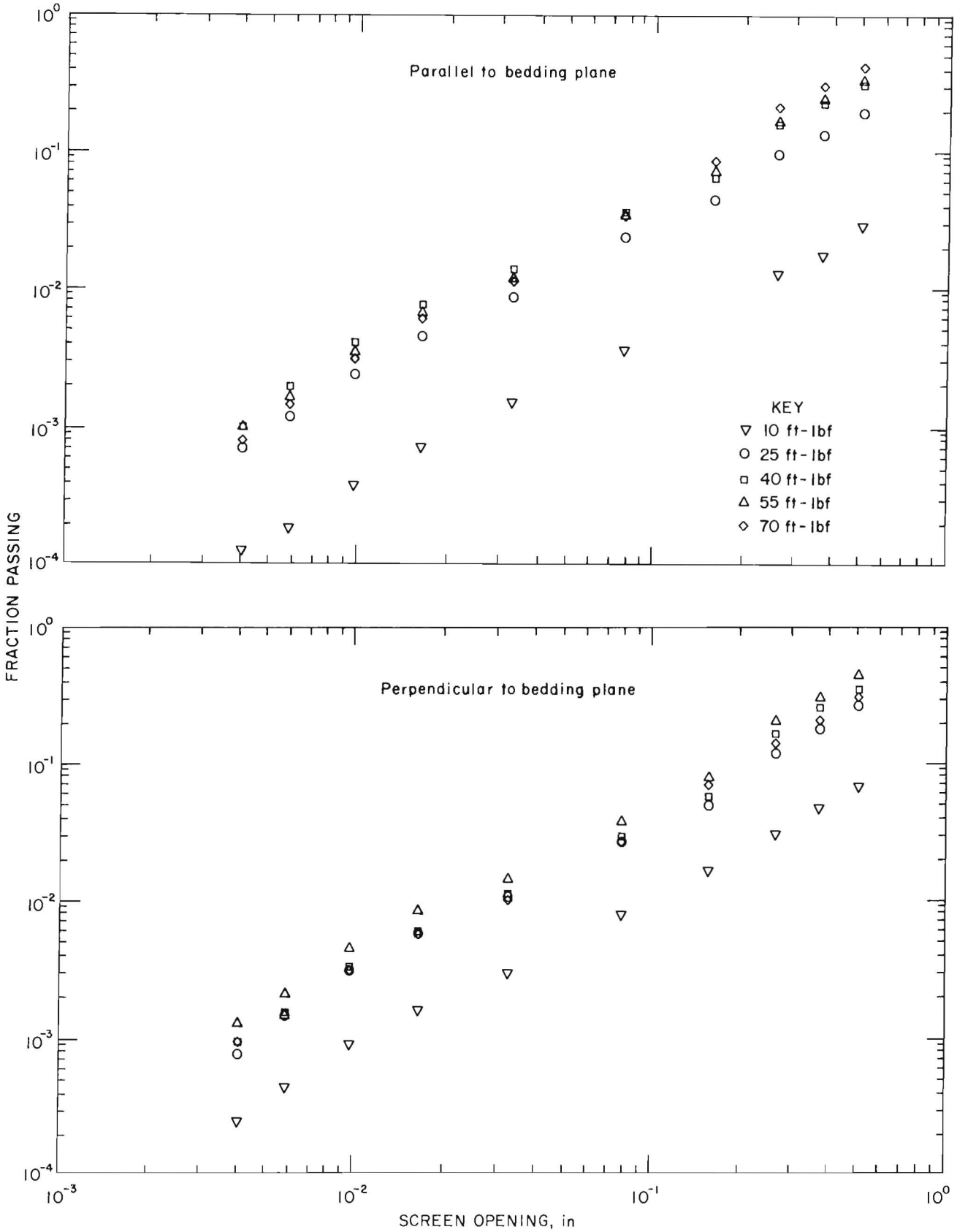

Figure 3.–Screening results for all input energies parallel (top) and perpendicular (bottom) to bedding plane.

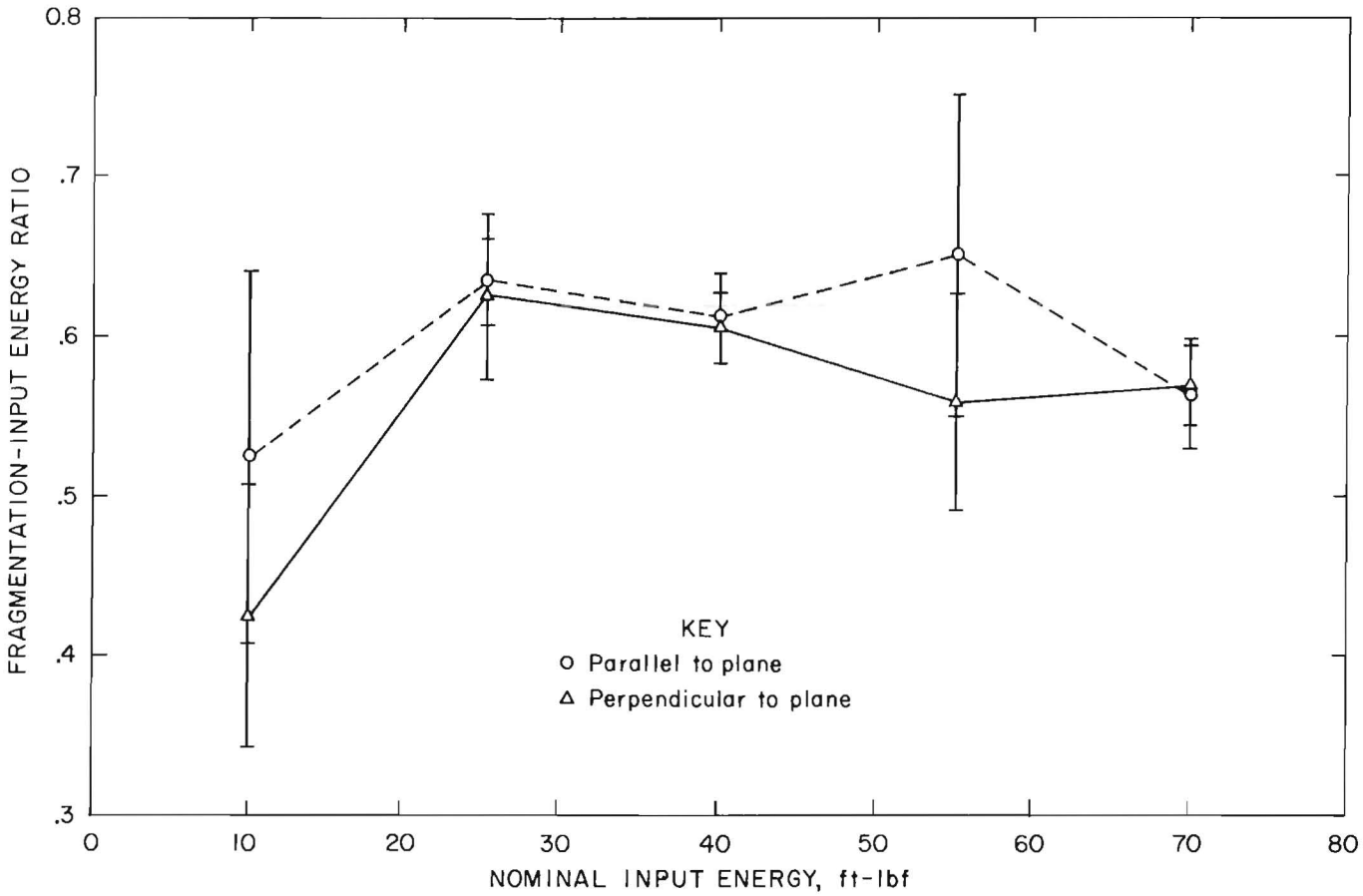

Figure 4.–Relationship between fragmentation-input energy ratio and nominal input energy.

As the input energy increased, energy absorbed during the fragmentation process increased (table 3). (The complete data set is shown in appendix A.) This was true for both directions of impact. An increase of input energy, from the lowest 10-ft•lbf input level to the highest 70-ft•lbf input level, produced a change of approximately 0.4 to 0.6 in the fragmenting-input energy ratio (fig. 4). The rise was followed by a slight decline above the 40-ft•lbf input energy level for impacts perpendicular and parallel to the bedding plane (table 3, fig. 4). Ratios for both impact directions remain approximately constant for input energies greater than 30 ft•lbf, taking into account the large standard deviations involved.

A statistically significant increase for particles passing 3/8-in mesh with increased energy input was indicated for the perpendicular impact (table 4, appendix G). Particulates passing 100 mesh followed the same trend, but there was consistency only for the lowest two input energy levels. Direction of impact did not show any statistically significant effect on the general increase of particulates passing 150-mesh openings, (table 2) with increased input energy (table 2). ARD on impact showed an increase with statistical significance for increased energy input (table 2, appendix H) for both directions of impact. There was no difference due to direction of impact. This suggests increasing fragmentation energy will increase respirable dust generation, but it also indicates that the generation is independent of the impact direction.

Table 4.–Parallel and perpendicular impact particles passing 3/8-in mesh, weight percent

Input energy, ft•lbf	Parallel		Perpendicular	
	Average	SD	Average	SD
10	0.05	0.06	0.018	0.005
25	.18	.07	.13	.05
40	.26	.11	.22	.06
55	.31	.05	.24	.12
70	.21	.06	.31	.06

SD Standard deviation.

The screened intermediate size fractions of 3, 5, 9, 20, 35, and 60 mesh were not analyzed for input energy level-direction effects because they have only minimal commercial significance. A summary of the raw data for these sizes is given in appendix B. The Weibull distributions for the sieved coal formed straight lines of similar slope on log-log plots for all energy levels and both bedding plane orientations. Summary plots of these data are shown in figure 3. These plots are useful in forecasting the particle size distribution for a given input energy. The plus 1/2-in size was ignored because of insignificant quantities involved.

Direction of impact did not contribute significantly to the ARD increase as input energy increased. The weight fraction from the minus 150-mesh fines showed a statistically significant increase with increased input energy regardless of impact direction except for an anomalous decline at the 70 ft•lbf input level (table 2). This percent of particulates below 11 μm was calculated on the basis of original sample weight and not on the basis of the minus 150-mesh fines weight. There was no statistically significant difference in fragments or dust formed due to direction of impact for all input energy levels. The analysis of variance (ANOVA) summary and the program for the dependent variables used to evaluate their overall trend significance are given in appendixes C and D, respectively.

Contrary to expectations, a comparison of the effects of impact direction failed to show significant difference in output energy distributions, size classifications, or dust generation properties. The Student's t-analysis described in appendix F was used to verify the significance of paired values. The results of the Student's t-analysis are contained in appendix G. The l0-ft•lbf tests produced little or no fragments and were excluded from the summary of Student's t-confidence level for 3/8-in screen size, 150-mesh screen size, and respirable dust on impact in appendixes G and H. Seven of these low-energy tests did not result in sample breakage.

SUMMARY

Perpendicular versus parallel direction of impact relative to a coal sample bedding plane at a given input energy had no significant effect upon dust, size distribution, and input versus output energy relationships. This observation held true for screened weight fractions, total dust, airborne respirable dust measured as a weight percent of the starting sample, and energy in terms of fragmentation energy or fragmentation energy to input energy ratios.

Energy consumed by the coal sample for fragmentation increased with an increase of input energy for both impact directions. The ratio of fragmentation energy to input energy remained constant for both sample orientations.

Respirable airborne dust increased with increased fragmenting energy. Direction of fragmenting energy in relation to the bedding plane had no significant effect upon useful coal size, amount of coal broken, or reduction of objectionable fines and dust.

The results of this laboratory study indicate that mine operators may disregard direction of cutting relative to the coal bedding plane as it relates to product size and dust. The mine operator should use the least cutting energy to produce the most plus 3/8-in-size coal. The lower energy favors minimum undesirable dust.

APPENDIX A.–ENERGY[1] DISTRIBUTION FOR PARALLEL AND PERPENDICULAR IMPACTS

Impact direction and pendulum arc, deg	Energy, ft•lb			Ratio[2]	Absorbed energy, ft•lbf
	Input	Retained	Fragmenting		
			10 ft•lbf NOMINAL INPUT ENERGY		
Parallel:					
10	10.22	1.38	6.10	0.597	2.74
10	10.15	.07	5.13	.505	4.95
10	10.21	.01	2.62	.257	7.58
10	10.19	.14	5.38	.528	4.68
9.8	9.84	.13	5.54	.563	4.18
9.9	10.0	1.59	6.03	.603	2.39
10	10.18	.08	6.33	.622	3.78
9.9	10.0	1.18	5.77	.577	3.05
9.9	10.05	.02	3.94	.392	6.09
10	10.10	2.55	6.08	.602	1.47
Average	10.09	.72	5.3	.52	4.1
SD	NAp	NAp	1.2	.12	NAp
Perpendicular:					
9.9	9.92	.10	5.10	.514	4.73
10	10.17	.04	3.58	.352	6.55
10	10.13	.07	4.09	.404	5.97
Average	10.07	.07	4.3	.42	5.8
SD	NAp	NAp	.8	.08	NAp
			25 ft•lbf NOMINAL INPUT ENERGY		
Parallel:					
15.7	24.98	2.64	16.29	0.652	6.05
15.7	25.06	3.95	14.55	.581	6.56
15.7	24.95	4.64	16.14	.647	4.17
15.7	24.82	4.42	16.17	.652	4.24
15.7	25.11	3.25	15.68	.625	6.17
15.8	25.12	3.19	16.54	.658	5.40
15.7	25.05	2.62	16.32	.652	6.11
15.7	25.0	4.35	15.40	.616	5.25
Average	25.01	3.6	15.9	.64	5.5
SD	NAp	NAp	.7	.03	NAp
Perpendicular:					
15.7	25.03	3.37	15.42	.616	6.24
15.7	24.93	2.05	15.68	.629	7.20
15.8	25.17	2.57	16.64	.661	5.96
15.7	24.89	2.09	17.12	.688	5.68
15.8	25.16	1.13	15.91	.632	8.12
15.7	24.99	2.62	15.81	.633	6.56
15.7	25.05	2.14	12.69	.507	10.22
15.7	24.91	3.20	5.85	.636	5.86
Average	25.02	2.4	15.6	.63	7.0
SD	NAp	NAp	1.3	.05	NAp
			40 ft•lbf NOMINAL INPUT ENERGY		
Parallel:					
20	40.44	11.02	23.41	0.579	6.01
20	40.17	7.24	23.53	.586	9.39
19.9	40.14	6.29	25.52	.636	8.32
19.9	39.76	5.19	26.44	.665	8.12
20.1	40.59	5.51	24.92	.614	10.16
20.0	40.29	10.42	23.78	.590	6.08
19.9	39.81	5.88	24.68	.620	9.26
19.9	40.08	5.43	25.18	.628	9.47
Average	40.16	7.1	24.7	.61	8.4
SD	NAp	NAp	1.1	.03	NAp
Perpendicular:					
20.0	40.27	6.86	25.0	.622	8.37
20.0	40.21	5.18	24.76	.616	10.26
19.9	39.92	6.90	22.49	.563	10.53
19.9	39.81	6.35	24.04	.604	9.42
19.9	40.06	5.93	23.92	.597	10.21
19.9	40.00	5.04	24.36	.609	10.60
19.9	39.94	4.59	24.47	.613	10.88
19.9	39.81	4.98	25.54	.642	9.30
Average	40.0	5.7	24.3	.61	10.0
SD	NAp	NAp	.9	.02	NAp

See explanatory notes at the end of tabulation.

APPENDIX A.–ENERGY[1] DISTRIBUTION FOR PARALLEL AND PERPENDICULAR IMPACTS–CONTINUED

Impact direction and pendulum arc, deg	Energy, ft•lb			Ratio[2]	Absorbed energy, ft.lbf
	Input	Retained	Fragmenting		
	55 ft•lbf NOMINAL INPUT ENERGY				
Parallel:					
23.4	55.06	10.33	44.05	0.800	0.68
23.4	55.04	12.79	31.51	.573	10.75
23.4	54.95	12.71	31.59	.575	10.65
23.4	54.84	8.24	33.03	.602	13.57
23.4	54.65	7.33	33.90	.618	13.62
23.4	55.24	9.33	45.75	.828	.15
23.5	55.26	9.68	35.07	.635	10.51
23.4	54.79	11.68	32.98	.602	10.13
Average	55.0	10.3	36.0	.65	8.8
SD	NAp	NAp	5.6	.10	NAp
Perpendicular:					
23.4	54.82	18.55	26.69	.4869	9.58
23.4	54.92	11.02	33.27	.6058	10.64
23.4	55.09	12.73	22.90	.5972	9.47
23.3	54.52	10.96	33.60	.6163	9.96
23.5	55.65	5.51	35.02	.6293	15.11
23.4	54.86	.03	24.02	.4378	30.82
23.4	54.93	13.45	31.92	.5811	9.55
23.4	54.80	5.93	29.52	.5387	19.35
Average	54.95	9.8	29.6	.56	14.3
SD	NAp	NAp	4.6	.07	NAp
	70 ft•lbf NOMINAL INPUT ENERGY				
Parallel:					
26.4	69.75	18.30	35.66	0.511	15.79
26.5	70.13	18.11	40.09	.572	11.92
26.5	70.12	17.34	37.45	.534	17.34
26.4	69.74	10.95	42.01	.602	16.78
26.4	69.97	14.91	38.20	.546	16.86
26.5	70.06	12.18	42.79	.611	15.09
26.4	69.95	12.10	41.19	.589	16.66
26.5	70.12	8.69	39.52	.564	21.90
Average	68.98	14.1	39.6	.57	16.5
SD	NAp	NAp	2.4	.03	NAp
Perpendicular:					
26.4	69.64	19.88	39.04	.561	10.72
26.5	70.05	15.41	42.75	.610	11.89
26.4	69.73	18.29	38.07	.546	13.37
26.4	69.89	13.87	40.31	.577	15.71
26.4	69.75	16.02	38.87	.557	14.87
26.5	70.08	11.06	39.94	.570	19.08
26.4	69.71	12.24	42.35	.608	15.12
26.5	70.11	12.14	38.94	.555	19.03
Average	69.87	14.9	40.0	.57	15.0
SD	NAp	NAp	1.7	.02	NAp

NAp Not applicable.
SD Standard deviation.
[1]Fragmenting energy–energy used in sample breakage; absorbed energy–backup bob response; retained energy–energy not spent in sample breakage or on backup bob response.
[2]Fragmenting energy to input energy.

APPENDIX B.–PARTICLE SIZE DISTRIBUTION FOR PARALLEL AND PERPENDICULAR IMPACTS, WEIGHT FRACTION PASSING[1]

Tyler screen	Parallel		Perpendicular		Parallel		Perpendicular	
	Average	SD	Average	SD	Average	SD	Average	SD
	10 ft•lbf				25 ft•lbf			
1/2 in	0.07	0.08	0.03	0.015	0.28	0.12	0.19	0.05
3/8 in	.05	.06	.018	.005	.18	.06	.13	.05
3 mesh	.03	.04	.014	.005	.12	.05	.096	.03
5 mesh	.02	.02	.032	.043	.050	.016	.046	.010
9 mesh	.009	.011	.004	.002	.028	.009	.025	.006
20 mesh	.003	.004	.0016	.0006	.011	.004	.009	.002
35 mesh	.002	.002	.0008	.0002	.006	.002	.005	.001
60 mesh	.001	.001	.0004	.0001	.0033	.001	.0026	.0005
100 mesh	.0005	.0007	.00020	.00006	.0016	.0005	.0013	.0003
150 mesh	.0003	.0005	.00013	.00006	.0008	.0003	.0007	.0002
	40 ft•lbf				55 ft•lbf			
1/2 in	0.35	0.15	0.31	0.07	0.45	0.7	0.33	0.15
3/8 in	.26	.11	.22	.06	.31	.05	.24	.12
3 mesh	.17	.07	.16	.05	.21	.04	.17	.08
5 mesh	.05	.02	.067	.013	.08	.02	.08	.03
9 mesh	.029	.009	.037	.006	.039	.007	.035	.009
20 mesh	.011	.004	.014	.003	.015	.002	.013	.003
35 mesh	.007	.002	.008	.001	.009	.002	.007	.002
60 mesh	.004	.001	.0042	.0009	.0047	.0010	.0037	.0009
100 mesh	.0017	.0006	.0022	.0005	.0022	.0010	.0017	.0003
150 mesh	.001	.0004	.0012	.0004	.0014	.0004	.0011	.0002
	70 ft•lbf							
1/2 in	0.33	0.10	0.42	0.08				
3/8 in	.21	.06	.31	.06				
3 mesh	.14	.04	.22	.03				
5 mesh	.07	.02	.09	.02				
9 mesh	.028	.005	.034	.008				
20 mesh	.011	.003	.012	.004				
35 mesh	.006	.002	.007	.003				
60 mesh	.0035	.0012	.0033	.0015				
100 mesh	.0017	.0006	.0016	.0008				
150 mesh	.0010	.0004	.0009	.0005				

SD Standard deviation.

[1]Sample weight entering given screen minus sample weight retained by that screen divided by starting sample weight (sum of fractions).

APPENDIX C.–ANOVA SUMMARY FOR DEPENDENT VARIABLES

	Direction	Energy	Iteration	Error
1/2-in mesh:				
Square, weight fraction passing:				
Sum	0.024	0.24	0.11	0.61
Mean	0.024	0.079	0.037	0.011
F-values	2.2	7.3	3.3	NA
Significance	NA	0.01	0.05	NA
Degree of freedom	1	3	5	56
3/8-in mesh:				
Square, weight fraction passing:				
Sum	0.0025	0.131	0.067	0.322
Mean	0.0025	0.044	0.022	0.0058
F-values	44	7.6	3.9	NA
Significance	NA	0.01	0.05	NA
Degree of freedom	1	3	3	56
100 mesh:				
Square, weight fraction passing:				
Sum	3.0×10^{-7}	3.1×10^{-6}	2.0×10^{-6}	1.6×10^{-5}
Mean	3.0×10^{-7}	1.0×10^{-6}	6.6×10^{-7}	2.9×10^{-7}
F-values	1.1	3.6	2.3	NA
Significance	NA	0.05	0.10	NA
Degree of freedom	1	3	3	56
150 mesh:				
Square, weight fraction passing:				
Sum	9.0×10^{-8}	1.7×10^{-6}	6.2×10^{-7}	6.5×10^{-6}
Mean	9.0×10^{-8}	5.6×10^{-7}	2.1×10^{-7}	1.2×10^{-7}
F-values	0.77	4.8	1.8	NA
Significance	NA	0.01	NA	NA
Degree of freedom	1	3	3	56
Dust on impact:				
1st set, 6 replications:				
Square, mg/m^3:				
Sum	160	3,000	220	3,700
Mean	160	1,000	73	93
F-values	1.7	11	0.78	NA
Significance	NA	0.01	NA	NA
Degree of freedom	1	3	3	40
2d set, 10 replications:				
Square, mg/m^3:				
Sum	1,100	62	30	3,100
Mean	1,100	31	15	57
F-values	19	0.55	0.27	NA
Significance	0.01	NA	NA	NA
Degree of freedom	1	2	2	54
ARD, 1.9 to 11 μm:				
Square, cumulative pct:				
Sum	1.1×10^{-7}	1.6×10^{-4}	1.3×10^{-5}	3.3×10^{-4}
Mean	1.1×10^{-7}	5.3×10^{-5}	$4.3 \times .0^{-6}$	5.9×10^{-6}
F-values	0.019	9.0	0.71	NA
Significance	NA	0.01	NA	NA
Degree of freedom	1	3	3	56
Energy consumed in sample breakage:				
Square, ft•lbf:				
Sum	43	5,200	120	460
Mean	43	1,700	40	8
F-values	5.2	210	4.9	NA
Significance	0.05	0.01	0.01	NA
Degree of freedom	1	3	3	56
Ratio:[1]				
Square:				
Sum	0.010	0.031	0.025	0.15
Mean	0.010	0.010	0.0082	0.0027
F-values	3.9	3.9	3.0	0.010
Significance	0.10	0.05	0.05	NA
Degree of freedom	1	3	3	56

ARD Airborne respirable dust.
NA Not available.
[1]Fragmenting energy to input energy.

APPENDIX D.–ANOVA PROGRAM[1]

```
10 DIM VL(2,3)
20 INPUT J
30 FOR I = 0 TO J - 1
40 READ VL(I,O),VL(I,I),VL(I,2),VL(I,3)
50 w = w + VL(I,O)
60 X = X VL(I,I)
70 Y = Y + VL(I,2)
80 Z = Z + VL(I,3)
85 QL = (VL(O,2) ^ 2 + VL(I,2). VL(2,2) ^ 2 + VL(O,3) ^ 2 + VL(I,3)
        ^ 2 + VL(2,3) ^ 2)
90 SE = SE + (VL(I,O) + VL(I,I)) ^ 2
95 QJ = (VL(O,O) Y 2 + VL(I,O) ^ 2 + VL(2,O). 2 + VL(O,I) ^ 2 + VL(I,I)
        ^ 2 + VL(2,I) ^ 2)
100 NEXT I
102 DATA 18.9472,12.3043,9.8718,2.0249
103 DATA 18.8503,10.2564,7.9301,4.5652
104 DATA 22.0896,11.9694,10.4543,6.6921
110 BK = 10
120 REM BK IS NO OF DATA IN BLOCK
130 BL = 6
140 REM BL IS NO OF BLOCKS IN RUN
150 DR = 3
160 REM DR IS NO OF BLOCKS FOR EACH DIR
170 Q = 54
180 REM Q IS RUNS-I-OF3-OF3-DFI
190 EY = 2
200 REM EY IS BLOCKS FOR EACH ENERGY INPUT
210 FR = 2
220 REM FR IS ENERGY DEG OF FREEDOM
230 IC = 2
240 REM IC IS INTERACTION FREEDOMS
250 REM DIR DEG OF FREEDOM IS ONE
260 GT = BK ^ (W + X)
270 SX = BK ^ QJ + (BK - 1) + QL
280 REM SX IS USED AS SXX
290 SD + (BK ^ (W. 2 + X ^ 2) / DR) - (GT ^ 2) / (BK * BL)
300 REM SD IS SS-DIR
310 SZ = (BK ^ 2) * SE / (BK * EY) - GT ^ 2 / (BK * BL)
320 REM SZ IS USED AS SS-ENERGY
330 SI = BK * (VL(O,O) ^ 2 + VL(I,O) ^ 2 + VL(2,O). VL(O,I) ^ 2 + VL
     (1,1) ^ 2 + VL(2,I) ^ 2) - (GT ^ 2) / (BK * BL) - SZ - SD
340 REM SI IS USED AS SS-INTERACT
350 SR = sx - (GT ^ 2) / (BK * BL) - SD - SZ - SI
360 REM SR IS USED AS SS-ERROR
370 ME = SR / Q
380 REM ME IS USED AS MS-ERROR
390 FD = SD / ME
400 REM FD IS DIR FOR F-TEST
410 NG = SZ / FR
420 REM NG IS USED AS MS-ENERGY
430 REM FR IS DEG OF FREEDOM FOR ENGY
440 FE = NG / ME
450 REM FE IS ENERGY F-TEST
460 MI = SI / IC
470 REM MI NIS MS-INTERACT, IC IS INTERACTION DEG OF FREEDOM
480 FI = MI / ME
490 REM FI IS INTERACTION F-TEST
500 REM MI IS MS-ERROR
510 PRINT FD,FE,FI,SD,SZ,SI,SR,SX,QL,QJ,SE,GT
520 END
```

```
18.9469455 = FD   .545259489 = FE   .268561078 = FI   1071.62903   61.6791687
30.3793411        3054.21105        19075.5781        339.356783    1602.1367
2983.87172        944.172
```

FD Direction - F-Test 18.947 Significant @ 0.01)
FE Energy - F-Test 0.545 Insignificant) > Dust significance
FI Interact - F-Test 0.269 Insignificant)

[1]Prepared by B. D. Hanson, physical scientist, Twin Cities Research Center, U.S. Bureau of Mines, Minneapolis, MN.

APPENDIX E.–INPUT ENERGY DETERMINATION FOR PENDULUM IMPACTOR[1]

Mass of striking pendulum and mounting arm, 341.6 lb.

Two steel sample plates, each nominally 2-1/2 by 2-1/2 by 1 in, 3.3 lb total.

Mass of receiving pendulum and mounting arm, 442.2 lb.

Length of striking pendulum measured from pivot center to center of percussion, 1.9677 ft (nominal 2 ft).

Bearing friction, 1.0±0.2 pct of input energy.

Example Input Energy Determination

Input energy = [1.9677 - (cos ϕ)(1.9677)]*341.6 or,

$$W = [L - (\text{Cos } \phi)(L)]M,$$

where W = Energy delivered, ft•lbf,

L = exact length of striking pendulum from center of pivot to center of percussion, ft,

cos ϕ = cosine function of the striking pendulum swing in degrees arc measured from the vertical rest position, to the lifted position,

and M = mass of striking pendulum, lb.

[1]Designed by R. C. Olson, mechanical engineer, Twin Cities Research Center, U.S. Bureau of Mines, Minneapolis, MN.

APPENDIX F.–STUDENT'S t-VALUES OF PAIRED DATA[1]

The calculated paired Student's t-value (T) indicates statistically significant differences between two given arithmetic average comparisons if the calculated t-value is not less than the handbook t-value for the same paired degrees of freedom at a given percent confidence level. The calculation equation is

$$T = \frac{(\bar{x}_2 - \bar{x}_1) - D_o}{\sqrt{\left[\frac{(n_2 - 1) \times s_2^2 + (n_1 - 1) \times s_1^2}{(n_2 + n_1 - 2)}\right] \times \left[\frac{1}{n_2} + \frac{1}{n_1}\right]}},$$

where D_o = null hypothesis set to zero for computing Student's t-value under the conditions described above,

$\bar{x}$ = arithmetic average of given data set; subscripts 1 and 2 indicate the first and second data sets being compared,

n = number of tests (replications) used,

$(n_2 + n_1 - 2)$ = degrees of freedom for a pair of data sets,

and s = standard deviation for a given data set.

$$s = \sqrt{\frac{\Sigma xi^2 - (\Sigma xi)^2/n}{n - 1}},$$

where Σx^2 = result of squaring each test result and summing the values,

and $(\Sigma xi)^2$ = result of summing a data set and squaring the sum.

[1]Mendenhall, W. Introduction to Linear Models and Analysis of Experiments. Wadsworth Publ., 1968, pp. 25-27.

APPENDIX G.–SUMMARY OF STUDENT'S t-NUMBERS AND CONFIDENCE LEVELS FOR 3/8-in AND I5O-MESH SCREENS

	3/8-in screen			150-in screen		
Impact energy . . ft•lbf . .	40	55	70	40	55	70
Parallel impact:						
25 ft•lbf:						
t-number	1.65	4.27	0.98	0.887	3.22	0.99
Confidence . . . . pct . .	NS	>95	NS	NS	>95	NS
40 ft·lbf:						
t-number	NAp	1.19	0.99	NAp	1.94	0.071
Confidence . . . . pct . .	NAp	NS	NS	NAp	>90	NS
55 ft·lbf:						
t-number	NAp	NAp	3.38	NAp	NAp	1.91
Confidence . . . . pct . .	NAp	NAp	>95	NAp	NAp	>90
Perpendicular impact:						
25 ft·lbf:						
t-number	3.15	2.41	6.87	3.5	3.10	0.78
Confidence . . . . pct . .	>95	>95	>95	>95	>95	NS
40 ft·lbf:						
t-number	NAp	0.42	2.92	NAp	1.205	1.8
Confidence . . . . pct . .	NAp	NS	>95	NAp	NS	>90
55 ft·lbf:						
t-number	NAp	NAp	1.48	NAp	NAp	1.08
Confidence . . . . pct . .	NAp	NAp	NS	NAp	NAp	NS

NAp Not applicable.
NS Not significant.

APPENDIX H.–SUMMARY OF AIRBORNE RESPIRABLE DUST GENERATED ON IMPACT

	1st set[1]				2d set[2]			
Impact energy . . . . ft•lb . .	25	40	55	70	25	40	55	70
Parallel impact:								
Average . . . . . mg/m^3 . .	7	9	14	22	NA	NA	12	10
SD . . . . . mg/m^3 . .	2	8	11	11	NA	NA	2	5
Perpendicular impact:								
Average . . . . . mg/m^3 . .	5	11	19	32	NA	NA	19	2
SD . . . . . mg/m^3 . .	3	6	15	12	NA	NA	8	10

NA Not available.
SD Standard deviation.
[1]6 replications.
[2]10 replications.

* U.S. GOVERNMENT PRINTING OFFICE: 611-012/00,105

INT.BU.OF MINES,PGH.,PA 28952